Translational Oncology
www.transonc.com

Volume 10 Number 4 August 2017 pp. 578–588 578

# The Role of Fibroblasts in Pancreatic Cancer: Extracellular Matrix Versus Paracrine Factors

**Louisa Bolm*, Simon Cigolla*, Uwe A. Wittel†, Ulrich T. Hopt†, Tobias Keck*, Dirk Rades‡, Peter Bronsert§,¶,#,1 and Ulrich Friedrich Wellner*,1**

*Department of Surgery, University of Luebeck, Luebeck, Germany; †Department of Surgery, Medical Center University of Freiburg, Faculty of Medicine, Germany; ‡Department of Radiation Oncology, University of Luebeck, Luebeck, Germany; §Institute of Surgical Pathology, Medical Center University of Freiburg, Faculty of Medicine, Germany; ¶Tumorbank Comprehensive Cancer Center Freiburg, Medical Center University of Freiburg, Faculty of Medicine, Germany; #German Cancer Consortium (DKTK) and Cancer Research Center (DKFZ), Heidelberg, Germany

## Abstract

*BACKGROUND AND AIM:* Desmoplasia is a characteristic feature and a suspected mechanism of tumor progression in pancreatic ductal adenocarcinoma (PDAC). Main constituents of the stroma involve cancer-associated fibroblasts (CAFs) and extracellular matrix (ECM). The aim of this study was to dissect the interaction of CAFs, ECM, and PDAC cells in both an *in vitro* setting and a large-scale clinical cohort study. *METHODS AND MATERIAL:* Patients operated for PDAC were identified from our prospectively maintained clinical database. A standard pathology protocol was applied for pancreatoduodenectomy specimens also assessing CAF activation as either CAF grade 0 or CAF grade +. Interaction between a spectrum of pancreatic cancer cell lines (PCCs) and mouse embryonic fibroblasts (NIH 3T3) was assessed in a conditioned medium experimental setup. *RESULTS:* One hundred eleven patients operated for PDAC from 2001 to 2011 were identified. Univariate analysis disclosed CAF grade + ($P = .030$), positive M status ($P < .001$), and lymph node ratio (LNR) > 0.1 ($P = .045$) to impair overall survival. Independent prognostic factors were CAF grade ($P = .050$) and positive M status ($P = .002$). CAF grade correlated with N status (CC = 0.206, $P = .030$), LNR (CC = 0.187, $P = .049$), tumor size (CC = −0.275, $P = .003$), and M status (CC = 0.190, $P = .045$). In the *in vitro* setting, paracrine effects of pancreatic cancer cell resulted in morphological activation of fibroblasts and tumor cell differentiation–dependent increase of fibroblast growth. Paracrine effects of poorly differentiated PCCs led to an upregulation of Vimentin in NIH 3T3 fibroblasts. Paracrine effects of fibroblasts on their part promoted cancer cell motility in all PCCs. As the second stromal component, fibroblast-derived ECM resulted in significantly decreased proliferation depending on density and led to upregulation of ZEB1 in poorly differentiated PCCs. *CONCLUSION:* In PDAC patients, positive CAF grading was identified as a negative prognostic parameter correlating with positive N status, high LNR, positive M status, and smaller tumor size. Whereas bilateral interaction of PCCs and CAFs promotes tumor progression, ECM poses PCC growth restrictions. In summary, our study discloses differential effects of stromal components and may help to interpret heterogeneous results of former studies.

*Translational Oncology (2017) 10, 578–588*

Address all correspondence to: Louisa Bolm, Department of Surgery, University of Luebeck, Ratzeburger Allee 160, D-23538, Luebeck, Germany.
E-mail: louisa.bolm@googlemail.com
[1] Contributed equally and share senior authorship.
Received 2 March 2017; Revised 19 April 2017; Accepted 24 April 2017


1936-5233/17
http://dx.doi.org/10.1016/j.tranon.2017.04.009

## Introduction

Characterized by a median 5-year overall survival of less than 5% and a high rate of early vascular, lymphatic, and perineural infiltration, pancreatic ductal adenocarcinoma (PDAC) is associated with dismal prognosis [1]. Aggressive PDAC biology is discussed as a main determinant of high rates of local and distant cancer cells dissemination [2].

Epithelial-to-mesenchymal transition (EMT) was studied in the past years as a concept to explain cancer cell invasion and formation of metastases [3,4]. EMT involves processes of cellular plasticity, namely, loss of epithelial differentiation, acquisition of mesenchymal characteristics, and cancer stem cell traits. Zinc finger E-box binding homeobox 1 (ZEB1) decisively promotes EMT mechanisms, leading to increased migration and invasiveness of PDAC cells [5]. As recently demonstrated, high expression of ZEB1 qualified as a negative prognostic factor in patients with PDAC or other adenocarcinoma [6,7]. As another feature of aggressive PDAC biology, cancer-associated fibroblasts (CAFs) play an important role in tumor progression [8–10]. In a reciprocal interaction network, PDAC tumor cells activate fibroblasts to CAFs, and CAFs for their part contribute to tumor growth, invasion, and the formation of distant metastases *in vitro* and in xenograft models [25]. CAF activation is common in PDAC and involves extensive desmoplasia with extracellular matrix (ECM) deposition [10,25]. We have previously demonstrated the impact of CAFs in PDAC as fibrotic stromal reaction at the mesopancreatic resection margin is of prognostic relevance [11]. Questioning the established concept of CAFs, recent studies suggest protective effects of desmoplastic stroma impeding tumor proliferation and invasion in PDAC [12,13]. Although the role of ZEB1 in the course of EMT and the role of CAFs, respectively, were studied *in vitro* and in xenograft models, clinical data remain rare. Furthermore, potential interlinks of CAFs, stromal components, and ZEB1 have not yet been investigated.

This study aims to characterize the role of fibroblasts in PDAC in both an *in vitro* setting and a large-scale clinical cohort study.

## Methods and Materials

### *Prognostic Analysis*

Patients operated for PDAC between 2001 and 2011 were identified from our prospectively maintained clinical database. During data acquisition, a standard pathology protocol was applied for pancreatoduodenectomy specimens. In the course of operation, the surgeon marked the resection margins. Specimens were assessed by an experienced pathologist, including measurement of macroscopic tumors or suspected areas. Tumor location, extent, and closest distances to the resection margins were documented. Pathologic reports comprised the macroscopic specimen description; diagnosis according to World Health Organization classification [14]; tumor grade according to Broders' classical grading system [15,16]; tumor stage according to the Union for international Cancer Control (pTNM); and microscopic status of the duodenal/gastric, jejunal, bilary and mesopancreatic resection margin (R0/R+). If there were concerns regarding margin or tumor-suspicious cells, additional pan-cytokeratin immunostaining was performed. Lymphatic invasion was classified as either present or absent (N0/N+). Lymph node ratio (LNR) was assessed as the number of involved lymph nodes in relation to the number of resected lymph nodes (minimum 12).

CAF activation grade was classified according to Ha et al. [17] as either high CAF+ (strong activation, immature stroma) or CAF 0 (weak activation, mature stroma). For CAF activation grade classification, hematoxylin/eosin-stained PDAC specimen slides were used. Mature tumor stroma was defined as tumor stroma including fibroblasts with small spindle cell morphology, a thin and wavy body structure, and a symmetric/parallel orientation. Immature tumor stroma included fibroblasts with plump spindle-shaped cell morphology and a prominent nucleus with prominent nucleoli and with random spatial orientation (Figure 1). The CAF grading was performed as an overall judgment of the tumor area in the PDAC tissue slides in 20-fold magnification. A value of more than 50% immature fibroblasts of all fibroblasts was considered as immature tumor stroma phenotype. CAF grade assessment was performed by one experienced pathologist (P.B.) and one histopathologically trained surgeon (U.F.W.) blinded to outcome parameters using a multiobserver microscope. The pathologist directed the object plate, and the grading was individually assessed and then compared slide by slide. In case of deviation, the respective slide was reevaluated and discussed.

### *Cell Culture*

A panel of pancreatic cancer cell lines (PCCs) was purchased from ATCC including highly aggressive cell lines with intrinsic ZEB1 expression (ASPC1, MIAPACA2, PANC1), as well as more

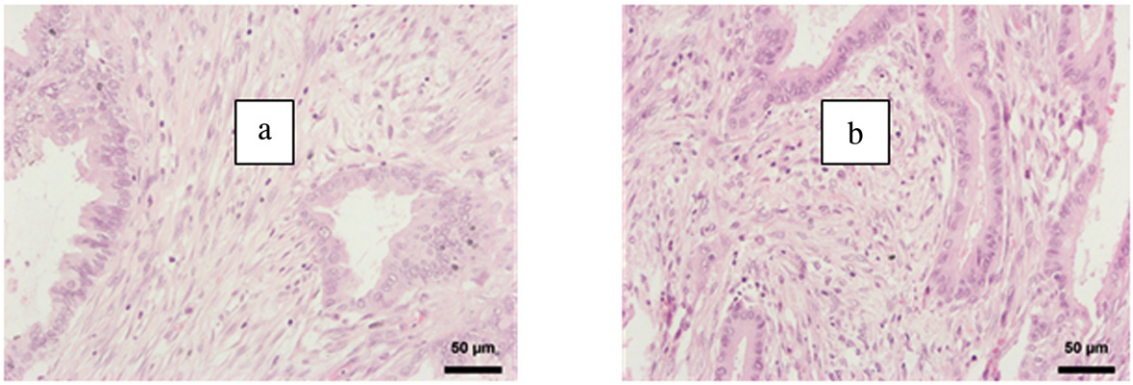


**Figure 1.** Fibroblast activation grade. As described previously [42], PDACs and CAFs were stained for hematoxylin-eosin. "Mature" fibroblasts were defined as thin and wavy fibroblasts with a "typical" slender and spindle-shaped morphology and symmetric/parallel orientation (A). "Immature" fibroblasts were defined as cells with prominent nucleoli and nucleus and a plump spindle-shaped morphology (B).

**Table 1.** Patient Baseline Parameters

| Parameter | *n*/Median | %/Range |
|---|---|---|
| All patients | 111 | 100 |
| CAF grade | | |
| Grade 0 | 14 | 13 |
| Grade + | 97 | 87 |
| Sex | | |
| Male | 58 | 52 |
| Female | 53 | 48 |
| Age in years | 67 | 30-89 |
| Resection | | |
| PPPD | 91 | 82 |
| Whipple | 14 | 13 |
| Total PE | 6 | 5 |
| PVR | 52 | 47 |
| Perioperative mortality | 4 | 4 |
| Tumor size in mm | 27 | 10-80 |
| T stage | | |
| T 1/2 | 13 | 12 |
| T 3/4 | 98 | 88 |
| M status | | |
| M 0 | 109 | 98 |
| M 1 | 2 | 2 |
| LNR | | |
| <0.1 | 52 | 47 |
| >0.1 | 59 | 53 |
| G grade | | |
| G1/2 | 66 | 59 |
| G3/4 | 45 | 41 |
| Lymphangiosis | 54 | 49 |
| Hemangiosis | 20 | 18 |
| Perineural invasion | 81 | 73 |
| Resection margin | | |
| Negative | 74 | 67 |
| Positive | 37 | 33 |

*PPPD*, pylorus-preserving pancreatoduodenectomy; *Whipple*, classical Whipple procedure; *Total PE*, total pancreatectomy; *PVR*, portal vein resection.

differentiated E-Cadherin–expressing cell lines (BXPC3 and HPAF2) [18]. The mouse embryonic fibroblast cell line NIH 3T3 was also purchased from the ATCC. NIH 3T3 cells represent an activated highly proliferative standard fibroblast cell line to investigate fibroblast-PDAC cell interaction.

All cells were cultured at 37°C in 5% $CO_2$ atmosphere in DMEM high-glucose medium with GlutamaX (Life Technologies #10566-032) containing 10% FBS (Life Technologies Standard FBS #10500-064).

### *PCC and Fibroblast Conditioned Medium Model*

Interaction between mouse embryonic fibroblasts (NIH 3T3) and PCC was evaluated applying a conditioned medium experimental setup. For generation of PCC–conditioned medium (PCC-CM), PCCs were grown until 70% confluence before transferring fresh medium (DMEM 10% FCS) and incubated for 72 hours. PCC-CM was then removed from PCCs, centrifuged at 1000 rpm for 5 minutes, sterile filtered (0.22 µm), and transferred to NIH 3T3 cells, which were previously seeded in standard culture flasks for 1 day prior and washed with PBS. Fresh PCC-CM was added every 3 days. NIH 3T3 cells were cultured in PCC-CM for 3 to 5 days until 70% confluence, and PCC-CM–treated and control NIH 3T3 cells were harvested after three times rinsing with PBS, centrifuged, and pelleted at 1000 rpm for 5 minutes. The same conditioned medium setup was performed for NIH 3T3–conditioned medium transferred to PCC.

### *Morphological Assessment In Vitro*

Morphological changes in NIH 3T3 cells were assessed at 70% confluence by calculating a length-width ratio (LWR) for 20 cells per

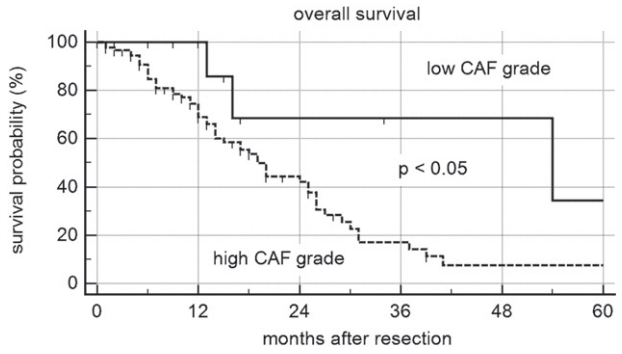


**Figure 2.** Univariate survival analysis CAF grade. *P* value derived from log-rank test.

microscopic visual field (20× magnifications). Four fields were assessed per flask. The freeware version of "Zeiss AxioVision" (https://www.zeiss.de) was used to evaluate the slides. Length and width of the cell body were measured in pixel, and a quotient was generated. *t* tests were performed comparing LWRs under standard condition to those in conditioned medium.

### *Cell Growth Assay*

Evaluating cell proliferation in control versus conditioned medium, 3-(4,5-dimethylthiazol-2-yl)-2,5-diphenyltetrazolium bromide (MTT) proliferation assays were performed. Cells were seeded in 6-well-plates at 150,000 cells/well in either conditioned or standard medium. Cell growth was measured using MTT assay as previously described [18]. After 3 days, MTT was added (5 mg/ml). Following an incubation of 4 hours, the medium was removed and the crystals were diluted in acidified isopropanol (0.04 N HCl). Absorption was measured at 570-nm emission. NIH 3T3 controls were cultured with 3-day self-conditioned medium.

### *Matrigel Transmigration Assay*

For measurement of the reciprocal paracrine invasion-promoting potential of NIH 3T3 cells and pancreatic cancer cells, Cultrex BME Cell Invasion Assay (Trevigen #3465-096-K) was performed according to the manufacturer's instructions. The upper chamber was coated with BME solution (10 mg/ml). 25,000 cells were seeded in the upper chamber in serum-free medium (DMEM) and standard medium with or without 25,000 cells were seeded in the lower chamber. After 72 hours, quantification of cells having migrated through the membrane pores was performed by fluorescent staining with Calcein AM solution (100 µl/well) as indicated by the manufacturer.

### *Polymerase Chain Reaction (PCR)*

Real-time PCR for analysis of mRNA expression was performed as previously described [19]. Isolation of mRNA was performed with RNeasy Plus Mini Kit (Qiagen) and subsequently transcribed to cDNA by Revert Aid First Strand cDNA Synthesis Kit (Fermentas). Relative expression was measured by quantitative real-time PCR (SYBR Green) in triplicates on a Roche LightCycler 96 using the Pfaffl method ##PMC55695## with beta-Actin as the reference gene transcript. We used mouse Vimentin primers (forward GCCCTCATTCCCTTGTTGCAG, reverse GACGAGGACACAGACCTGGTA).

### *ECM Assay*

NIH 3T3 fibroblast-derived matrix was prepared as previously described [20]. Pancreatic cancer cells (150,000 cells/well) were

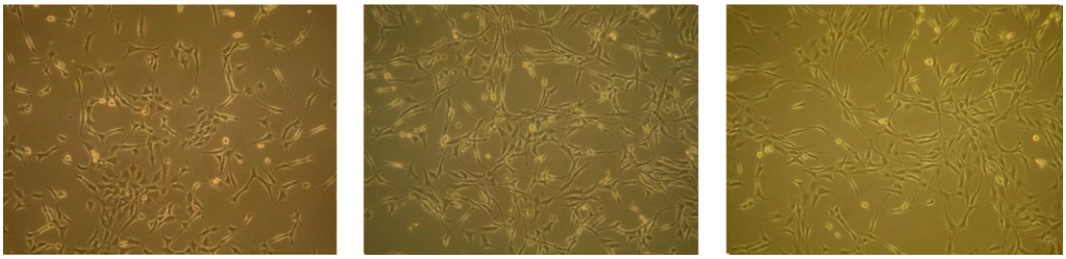

a b c

NIH 3T3 cells treated with standard medium (a), CM by HPAF 2 (b), CM by PANC 1 (c). Photos were taken at 20-fold magnification two days after transfer of conditioned medium to NIH 3T3 cells. Length-width-ratio (LWR) was calculated measuring length and width of the cell body in pixel and a quotient was generated.

Length-Width-Ratio (LWR) of NIH 3T3 cells treated with PCC-conditioned medium

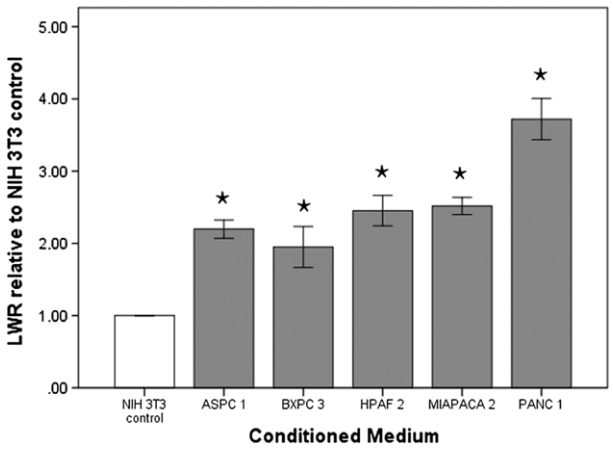


| Derivation of CM | p-value |
|---|---|
| NIH 3T3 control (self-conditioned) | |
| HPAF 2 | **0.001** |
| PANC 1 | **0.001** |
| BXPC 3 | **0.001** |
| MIA PACA 2 | **0.001** |
| ASPC 1 | **0.001** |

Diagrams depict mean and error bars (95% confidence level) from n=20 measurements in 4 microscopic high power fields. * p<0.05 in two-sided t-test compared to NIH 3T3 control. Abbreviations: CM: conditioned medium, PCC: pancreatic cancer cells, LWR: length-width ratio, PDAC: pancreatic ductal adenocarcinoma

**Figure 3.** Fibroblast morphology in medium conditioned by pancreatic cancer cells (PCC-CM).

seeded in ECM established over 3 days and over 7 days, with standard cell culture plastic as the control. MTT proliferation assay and mRNA expression analysis were performed as described above.

### *Statistics*

Data collection and statistical analysis were performed with IBM SPSS Version 21 (SPSS Inc., Chicago, IL). Scale variables were expressed as median and range, categorical parameters by cross-tabulation, and percentages and survival data by Kaplan-Meier method. For statistical testing, Student *t* test, Spearman rank correlation, log-rank test, and a multivariate Cox proportional hazard model were applied.

## Results

### *Clinical Relevance of CAF Activation Grade*

One hundred eleven patients with PDAC were identified from our prospectively maintained database and included in this study. Ninety-one patients received a pylorus-preserving pancreatoduodenectomy, 14 were operated on by classical "Whipple" procedure, and only 6 underwent total pancreatectomy. Forty-seven percent of the patients had portal vein resections. Of 111 patients with PDAC, 88% were diagnosed as T3/4, and still a majority presented with an LNR higher than 0.1 (53%). A percentage of 33% underwent a margin positive resection (R+). The CAF grade classification revealed a percentage of 87% being CAF grade +. Patient characteristics are depicted in Table 1.

Univariate analysis by Kaplan-Meier disclosed CAF grade + ($P$ = .030), positive M status ($P$ < .001), and LNR > 0.1 ($P$ = .045) as negative prognostic factors. Median survival in patients with CAF grade 0 versus CAF grade + was 54 versus 19 months, respectively (Figure 2). Median LNR was 0.10, resulting in median survival of patients with an LNR < 0.1 versus patients with an LNR > 0.1 of 26 versus 19 months, respectively. All parameters with $P$ < .05 on univariate analysis (CAF grade, LNR, M status) were included in a

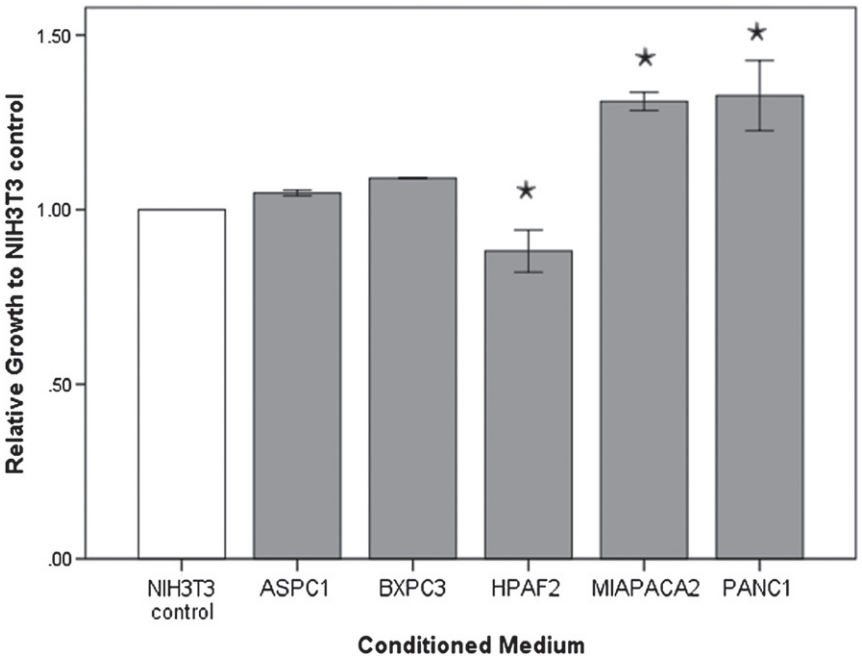


| Derivation of CM | p-value |
|---|---|
| ASPC 1 | 0.240 |
| BXPC 3 | 0.253 |
| HPAF 2 | **0.002** |
| MIAPACA 2 | **0.023** |
| PANC 1 | **0.001** |

NIH 3T3 fibroblast proliferation in PCC-conditioned medium. Cell growth was quantified by MTT proliferation assays. NIH 3T3 growth in PCC-conditioned medium was measured relative to NIH 3T3 growth in standard control medium. The diagram depicts mean and error bars (95% confidence level) of n=4 measurements. * p<0.05 in two-sided t-test relative to standard medium NIH 3T3 control. Abbreviations: CM: conditioned medium, PCC: pancreatic cancer cells

**Figure 4.** Proliferation assay of NIH 3T3 cells in PCC-CM.

Cox proportional hazard model. The only independent prognostic factors were M status ($P$ = .002) and CAF grade ($P$ = .050).

### *Correlation of CAF Activation with Histopathologic Parameters*

Bivariate correlation (Spearman) disclosed significant positive correlation of CAF grade + and positive N status (CC = 0.206, $P$ = .030). Furthermore, CAF grade correlated with LNR (CC = 0.187, $P$ = .049) as well as M status (CC = 0.190, $P$ = .045) and tumor size (CC = −0.275, $P$ = .003).

### *Experimental Effects of Cancer Cells on Fibroblasts*

The activation of quiescent fibroblasts comprises the transformation of a multispine phenotype to spindle-like and more elongated cell body characteristics. Morphology of NIH 3T3 fibroblasts treated with medium conditioned by pancreatic cancer cells (PCC-CM) was quantified by calculating LWRs; a quotient of length and width of the cell bodies was calculated. LWRs were significantly higher, describing a more elongated morphology in NIH 3T3 cells cultivated in PCC-CM as compared to those receiving standard medium ($P$ = .001, Figure 3).

To assess the influence of PCC-CM on NIH 3T3 fibroblast proliferation, MTT assays were performed. PCC-CM derived from MIAPACA 2 and PANC 1 cell lines significantly increased cell growth in NIH 3T3 fibroblasts. Fibroblast growth was slightly increased by ASPC1-CM and BXPC3-CM; however, the effect did not reach statistical significance. PCC-CM by HPAF2 cell line significantly reduced cell growth in fibroblasts (Figure 4). Overall, the effects of PCC on fibroblast growth were weak, possibly due to intrinsic high proliferation rates of NIH 3T3 cells only sparsely alterable. Fibroblast conditioned medium did not impact pancreatic cancer cell growth in the MTT assay (data not shown).

mRNA expression levels of Vimentin as a marker of CAF activation were analyzed in NIH 3T3 cells treated with PCC-CM. Fibroblasts were cultivated for either 3 days (short time) or 30 days (long time) in PCC-CM before isolation of mRNA. mRNA expression level of Vimentin was significantly increased in NIH 3T3 cells treated with PCC-CM from aggressive undifferentiated PCC with high intrinsic ZEB1 expression (ASPC 1, PANC 1) but significantly decreased in those treated with PCC-CM derived from well-differentiated cell lines (BXPC 3, HPAF 2). This effect was more pronounced in NIH 3T3 fibroblasts cultivated in PCC-CM (PANC 1, HPAF 2) for a longer period (30 days) (Figure 5).

### *Paracrine Effects of Fibroblasts on Cancer Cells*

For evaluation of invasion-promoting effects of NIH 3T3 fibroblasts on PCC, cell invasion assays were performed. Cultivating

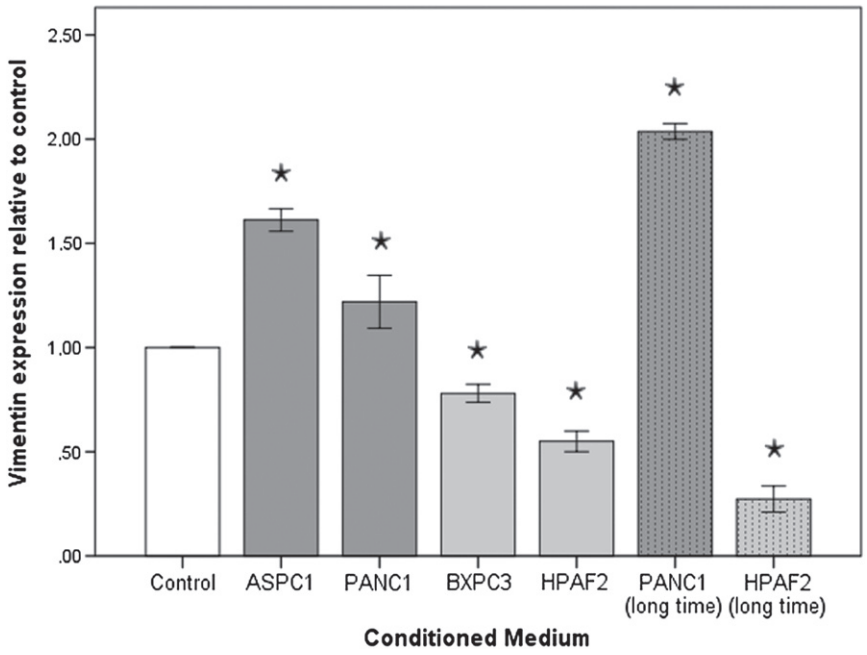


| PCC | p-value |
|---|---|
| ASPC 1 | **<0.001** |
| BXPC 3 | **<0.001** |
| HPAF 2 | **0.001** |
| PANC 1 | **0.029** |
| HPAF 2 LT | **<0.001** |
| PANC 1 LT | **<0.001** |

m-RNA expression levels of Vimentin in NIH 3T3 fibroblast grown in PCC-conditioned medium. NIH 3T3 were treated with conditioned medium derived from aggressive highly ZEB1 expressing cell lines (dark grey bars), less aggressive cell lines with low ZEB1 expression levels (light grey bars) for 3 days (short term) or 30 days (long term, dotted bars). Vimentin expression was measured by quantitative real time PCR. The figure shows baseline Vimentin expression in NIH3T3 fibroblasts relative to Vimentin expression in NIH 3T3 fibroblasts treated with conditioned medium. The diagram depicts mean and error bars (95% confidence level) of n=4 measurements. * $p<0.05$ in two-sided t-test relative to standard medium NIH 3T3 control.
Abbreviations: CM: conditioned medium; PCC: pancreatic cancer cells

**Figure 5.** Vimentin mRNA expression levels in NIH 3T3 cells treated with PCC-CM.

NIH 3T3 fibroblasts in the lower chamber and PCC in the upper chamber, PCC migration through the separating Matrigel and filter membrane was measured and compared to PCC invasion rates without NIH 3T3 fibroblasts cultivated in the lower chamber. Paracrine effects of NIH 3T3 fibroblasts resulted in significantly increased migration in all PCCs (Figure 6). Pancreatic cancer cells did not enhance NIH 3T3 fibroblast invasion.

### *Effects of Fibroblast-Derived ECM on Cancer Cells*

To assess interaction of PCC and ECM, PCCs were seeded in ECM established by NIH 3T3 fibroblasts over 3 days (moderate ECM) and over 7 days (extensive ECM). In moderate ECM, PCC growth was strongly and significantly reduced in all PCC cell lines, and in extensive ECM, the effect was even stronger (Figure 7).

mRNA expression of the EMT marker ZEB 1 was measured in cancer cells cultivated on fibroblast-derived ECM. After 4 days, ZEB 1 expression was significantly increased over control in all PCC cell lines except from BXPC3. This effect was especially pronounced in aggressive undifferentiated PCC with a high intrinsic ZEB1 expression (ASPC 1, PANC 1) (Figure 8).

## Discussion

PDAC is associated with poor prognosis, and the majority of patients initially present with locally advanced or metastasized tumors. Complete resection remains the only curative option in PDAC; however, early systemic disease is common [1,2]. Several prognostic factors in PDAC have been identified in recent years. Lymph node metastasis, high LNR, and distant metastasis are well-established negative prognostic factors representing advanced tumor cell spread and indicating aggressive tumor biology in PDAC [21,22]. Our study is the first to demonstrate CAF grade as an even more important

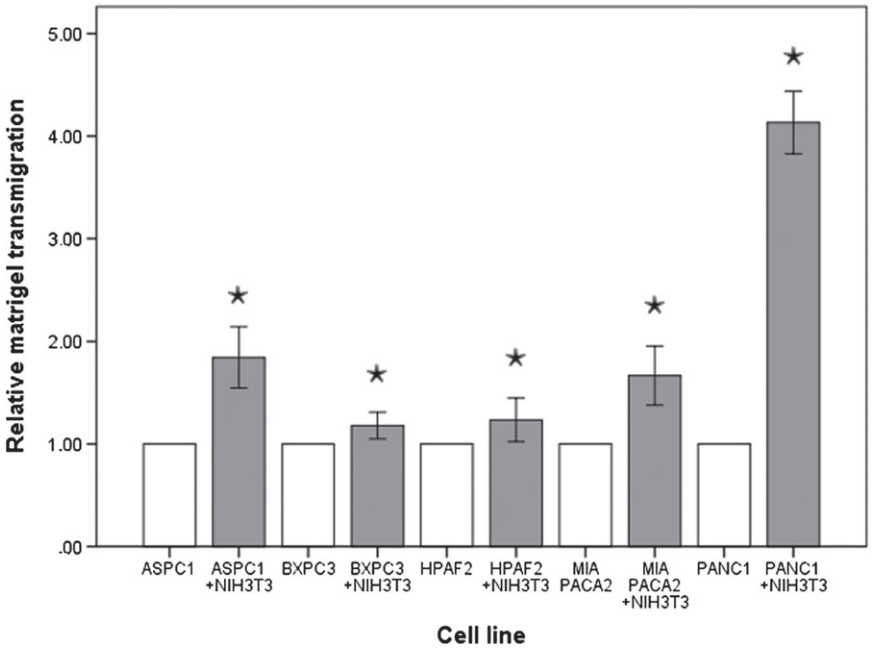


| CIA upper chamber | CIA lower chamber | p-value |
|---|---|---|
| ASPC 1 | | |
| ASPC 1 | NIH 3T3 | **0.001** |
| BXPC 3 | | |
| BXPC 3 | NIH 3T3 | **0.001** |
| HPAF 2 | | |
| HPAF 2 | NIH 3T3 | **0.039** |
| MIAPACA 2 | | |
| MIAPACA 2 | NIH 3T3 | < **0.001** |
| PANC 1 | | |
| PANC 1 | NIH 3T3 | < **0.001** |

Cell invasion assay was performed seeding pancreatic cancer cells in serum free medium (upper chamber). The lower chamber contained only attractant medium (medium, 10% FCS) in the control group. The paracrine effects of additionally seeding NIH 3T3 in the lower chamber were quantified relative to the control group. The diagram depicts PCC baseline matrigel transmigration as compared to PCC matrigel transmigration effected by NIH 3T3 fibroblasts in the lower chamber. Mean and error bars (95% confidence level) are derived from n=4 measurements. * $p < 0.05$ in a two-sided t-test compared to control. Abbreviations: PCC: pancreatic cancer cells, CIA: cell invasion assay

**Figure 6.** Paracrine effects of NIH 3T3 fibroblasts on PCC Matrigel transmigration.

prognostic factor compared to established prognostic factors such as LNR. In our study, only M status qualified as additional independent prognostic factor. Morphologically high activation of CAF/immature tumor stroma was associated with reduced overall survival in PDAC patients. An emerging body of evidence suggests a decisive role of tumor stroma in tumor progression, tumor cell dissemination, and metastasis in PDAC [8–10]. High CAF activation grade was associated with positive N status, high LNR, positive M status, and small tumor size. Consequently, a CAF-driven local and systemic tumor cell dissemination occurring already at an early stage of tumor growth may be postulated in tumors with high CAF grade. We chose to classify CAF activation as previously described by Ha et al. [17]. The authors defined the CAF grading for esophageal cancer and observed CAF grade + in 45% of the examined specimens. There are some aggressive subtypes known for esophageal cancer, and 5-year overall survival rates vary around 15% to 25% [17,43]. However, PDAC remains the most aggressive solid cancer type, displaying 5-year survival rates of only 5% [1]. Consequently, we assumed a higher tumor-cell–driven activation of CAFs in this context. Additionally, although desmoplasia can be a feature of esophageal cancer, it is much more characteristic for PDAC explaining a CAF grade + rate as high as 87% in our study.

To further investigate underlying mechanisms, we aimed to characterize reciprocal effects of CAF and PDAC cells in an experimental model.

Interaction of CAF and PDAC cells was described in several studies mainly based on *in vitro* or xenograft models. Physiologically, fibroblasts contribute to wound healing and formation of granulation tissue. In this process, fibroblasts are transformed to activated myofibroblasts characterized by stress fibers and extensive ECM production [23]. PCC may activate the transformation of fibroblasts to CAFs and enhance their proliferation [30,31]. In this process,

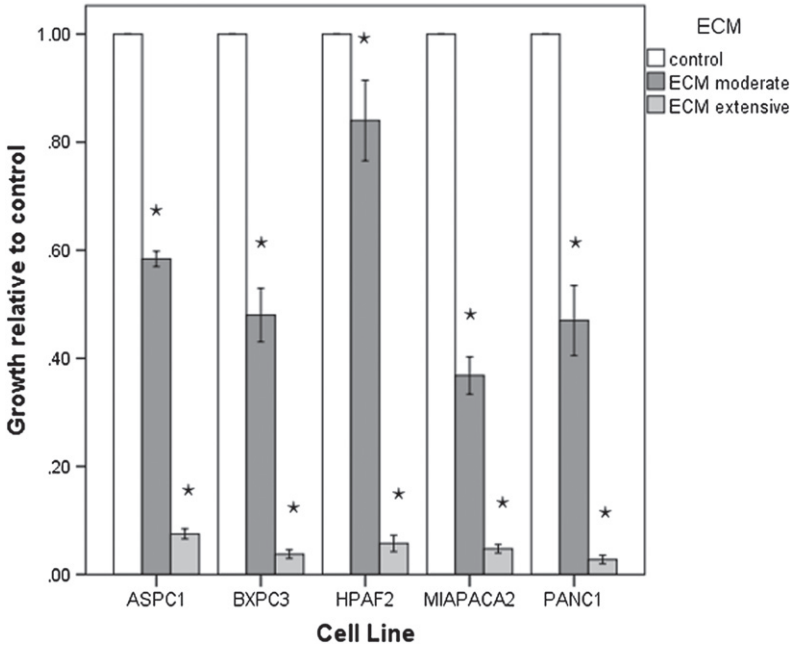


Growth relative to control in moderate density ECM (established by NIH 3T3 fibroblasts over 3 days)

| PCC | p-value |
|---|---|
| ASPC 1 | **<0.001** |
| BXPC 3 | **<0.001** |
| HPAF 2 | **<0.001** |
| MIAPACA 2 | **<0.001** |
| PANC 1 | **<0.001** |

Growth relative to control in high density ECM (established by NIH 3T3 fibroblasts over 7 days)

| PCC | p-value |
|---|---|
| ASPC 1 | **<0.001** |
| BXPC 3 | **<0.001** |
| HPAF 2 | **<0.001** |
| MIAPACA 2 | **<0.001** |
| PANC 1 | **<0.001** |

PCC proliferation in moderate and extensive ECM. Cell growth was quantified by MTT proliferation assays. PCC growth in ECM was measured relative to growth without ECM in standard control medium. ECM was established by NIH 3T3 fibroblasts over 3 days (moderate ECM) and over 7 days (extensive ECM). The diagram depicts mean and error bars (95% confidence level) of n=4 measurements. * $p<0.05$ in two-sided t-test relative to standard medium NIH 3T3 control.
Abbreviations: ECM: extracellular matrix, PCC: pancreatic cancer cells

**Figure 7.** Proliferation of PCC in moderate and extensive ECM.

resident mesenchymal pancreatic stellate cells or fibroblasts of the bone marrow are recruited by PCC [10,24]. Activated CAFs are characterized by a spindle-like morphology. In our study, we confirmed these morphological activation changes in fibroblasts treated with PCC-CM. Increased fibroblast proliferation rates by PCC-CM treatment were observed for PCCs of poor differentiation. In contrast, fibroblast proliferation was reduced by conditioned medium of a well-differentiated cell line. However, this effect was weak, possibly due to intrinsic high proliferation rates of NIH 3T3 cells only sparsely alterable. Additionally, fibroblast starvation might be an effect in this context. A starvation effect was not definitely controllable in our *in vitro* model as it would require frequent medium change counteracting the conditioning process. Starvation of PDAC cells as a result of desmoplasia might be present *in vivo* as well, as proposed by Sousa et al. 2014 [42]. The authors demonstrated a reprogramming in PDAC metabolism leading to augmented nutrient acquisition and postulated this effect to be a result of desmoplasia and hypovascularization frequently present in PDAC. Consequently, a certain amount of PDAC cell starvation might mirror *in vivo* conditions.

Only few studies have investigated the effect of PCC on Vimentin expression in CAF. Vimentin as a mesenchymal marker is consecutively expressed in CAF. A recent study showed upregulation of Vimentin expression as indicative for CAF activation and aggressive

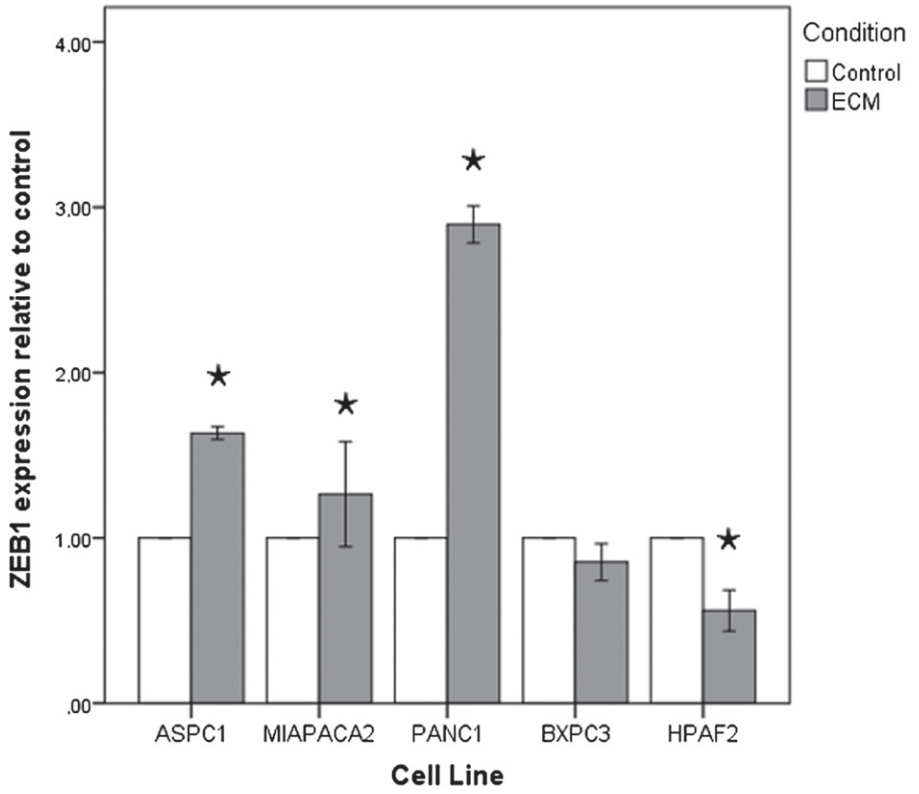


| PCC | p-value |
|---|---|
| ASPC 1 | **<0.001** |
| MIAPACA 2 | **0.023** |
| PANC 1 | **<0.001** |
| BXPC 3 | 0.057 |
| HPAF 2 | **0.004** |

ZEB1 mRNA expression levels of PCC seeded in NIH 3T3 fibroblast derived ECM. ZEB1 mRNA expression was measured by quantitative real time PCR. ZEB1 expression in PCC seeded in ECM is shown relative to baseline ZEB1 expression levels of respective PCC lines. The diagram depicts mean and error bars (95% confidence level) of n=4 measurements. * $p<0.05$ in two-sided t-test relative to standard medium NIH 3T3 control.
Abbreviations: ZEB1: zinc finger e-box binding homeobox 1, ECM: extracellular matrix, PCC: pancreatic cancer cells

**Figure 8.** ZEB1 mRNA expression in pancreatic cancer cell lines in the absence versus presence of ECM established by NIH 3T3 cells.

biology [32]. In a study by Brentnell et al., Vimentin expression in CAF was associated with enhanced cancer cell invasion [33]. In a co-cultivation *in vitro* model, paracrine effects of hepatocellular carcinoma cells led to upregulation of Vimentin in fibroblasts [34]. In our study, fibroblasts treated with PCC-CM by poorly differentiated PCCs showed high expression levels of Vimentin. Well-differentiated cell lines, however, reduced Vimentin expression levels. However, there was no strong PCC-mediated effect on fibroblast growth, and proliferation changes were not mirrored by Vimentin expression.

An emerging body of evidence is indicating tumor-promoting effects of CAFs on PCCs [25–29]. As described by Kalluri et al., CAFs reflect a heterogeneous and plastic population capable of reprogramming the tumor environment and even potentially impacting therapy outcome [25]. CAFs secrete paracrine factors promoting tumor growth, PCC survival, and formation of metastasis [10,26,30]. In our experimental model, we confirmed an invasion-promoting paracrine effect of NIH 3T3 fibroblasts on PCCs of all differentiation types. These *in vitro* results correspond well with our clinical analysis demonstrating an association of positive CAF grade and local and systemic tumor cell spread in terms of positive N status, high LNR, and positive M status.

Desmoplasia is a characteristic feature of PDAC and constitutes up to 90% of the tumor volume. Mainly ECM, but also CAF, immune cells and vascular components form the desmoplastic microenvironment [35,36]. In our study, ECM posed a proliferation-restricting effect on PCC. Simultaneously, EMT-marker ZEB1 was upregulated in poorly differentiated PCCs. The concept of EMT was established in the past years to explain mechanisms of cancer cell proliferation and motility [3,4,38]. EMT comprises various transformation processes of cancer cells involving loss of epithelial differentiation

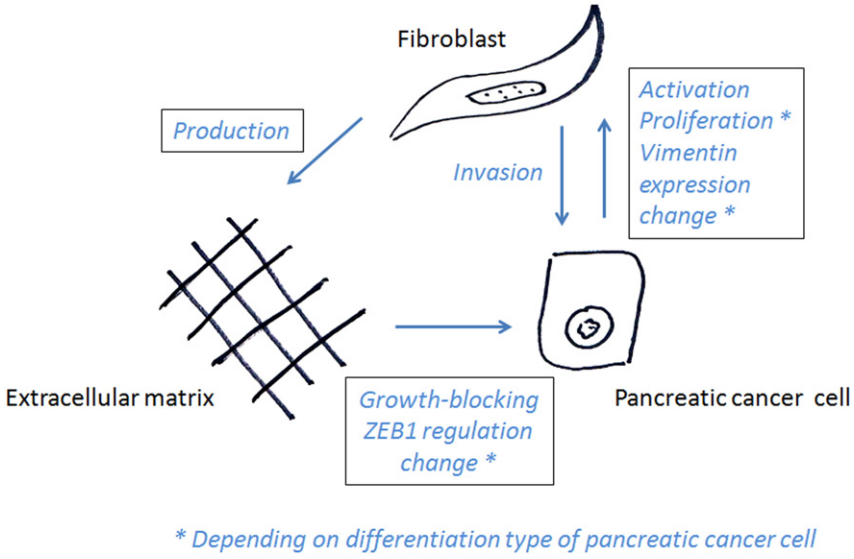


**Figure 9.** Proposed stroma interaction model.

and acquisition of a mesenchymal phenotype able to migrate. ZEB1 expression was identified as a hallmark of EMT [6,19,40]. ZEB1 causes major gene expression changes in epithelial cells by binding to specific DNA sequences (E-boxes and Z-boxes) in the promoter region of its target genes executing mainly transcriptional repressive functions [39]. ZEB1 upregulation leads to decreasing expression levels of epithelial marker E-Cadherin and a partial or complete loss of typical epithelial cell characteristics such as cell polarity and cell-cell adhesion [40]. The role of EMT in the interaction of tumor cells and ECM is not yet well examined for PDAC. Brabletz et al. investigated the interaction of colorectal cancer cells and collagen 1 matrix and found EMT features such as downregulation of E-Cadherin in formerly well-differentiated cell lines [37]. However, tumor cell proliferation was decreased. This corresponds very well with the ECM-promoted limitation in tumor cell growth and a simultaneous upregulation of ZEB1. Our study is the first to demonstrate a similar EMT-promoting effect of ECM in undifferentiated aggressive PDAC cells.

In our study, rates of portal vein resection were as high as 47%. A recent study by Lapshyn et al. [41] demonstrated histopathological portal vein invasion as a negative prognostic factor associated with aggressive biological features such as downregulation of E-Cadherin and high CAF activation [41]. In the patients showing portal vein invasion, the authors demonstrated higher rates of margin positive resections. Consequently, a clinically relevant interlink of CAF activation, aggressive EMT-related biological markers, and portal vein invasion might be postulated.

Recent studies present conflicting results concerning the role of PDAC stroma provoking a controversial debate. A study by Rhim et al. has raised concerns regarding desmoplasia-promoted tumor progression and invasion in PDAC [12]. By deletion of sonic hedgehog ligand, the authors generated a PDAC mouse model expressing reduced levels of fibroblasts and stroma. Shh-deficient tumors showed undifferentiated histology as well as an increase in vascularization and proliferation, leading to overall reduced survival. Another study by Özedemir et al. demonstrated that complete abrogation of myofibroblasts and desmoplastic stroma in PDAC led to faster tumor progression [13]. In our study, we found ECM-mediated limitation of PCC proliferation in the *in vitro* approach and mature dense stroma qualified as positive prognostic factor in the clinical investigation. It might consequently be speculated that unrestrained tumor growth and PCC invasion observed by Rhim et al. and Özdemir et al. could be mainly attributable to the absence of growth-restricting CAF-derived ECM.

We propose a PDAC stroma model differentiating paracrine and ECM-mediated CAF effects (Figure 9). Our model suggests a limitation of PCC growth by contact with fibroblast-derived ECM. Therefore, apart from constituting a physical barrier to tumor cell invasion, fibroblast-derived ECM seems to strongly inhibit PCC growth. On the other hand, paracrine factors secreted by fibroblasts seem to increase local invasion of tumor cells. These experimental observations are confirmed by our clinical investigation: immature stroma is a surrogate parameter of low ECM production, but high paracrine activity correlated with poor prognosis.

This heterogeneity of CAF functions has also been highlighted in a recent study by Öhlund et al. The authors describe a myofibroblast CAF subtype producing ECM, opposed to an inflammatory CAF subtype secreting tumor-promoting soluble factors [35]. Further characterization of distinct CAF- and stroma-mediated effects as well as identification of stroma and CAF subtypes may contribute to finally developing stoma-targeted therapeutic options in PDAC.

It has to be mentioned that the presented study has several limitations. The clinical approach was of retrospective nature. The *in vitro* setting is limited to single aspects of the complex CAF-PCC interaction network and can only be an approximation of the *in vivo* microenvironment.

## Conclusion

In summary, we demonstrate high CAF activation and immature stroma as negative prognostic factors associated with local and systemic cancer cell dissemination in PDAC. PCC-mediated activation of fibroblasts to CAFs was pronounced in poorly differentiated PCC lines. ECM mediated restriction of PCC proliferation and upregulation of the EMT marker ZEB1, whereas secreted CAF factors promote cancer cell invasion in a paracrine way. This antagonism may also help to explain seemingly conflicting results of former studies.

## Conflict of Interest

On behalf of all authors, the corresponding author states that there is no conflict of interest related to this study.

## References


[1] Lillemoe KD, Yeo CJ, and Cameron JL (2000). Pancreatic cancer: state-of-the-art care. *CA Cancer J Clin* **50**(4), 241–268.

[2] Bramhall SR, Allum WH, Jones AG, Allwood A, Cummins C, and Neoptolemos JP (1995). Treatment and survival in 13560 patients with pancreatic cancer, and incidence of the disease, in the West Midlands: an epidemiological study. *Br J Surg* **82**, 111–115.

[3] Brabletz S, Bajdak K, Meidhof S, Burk U, Niedermann G, Firat E, Wellner U, Dimmeler A, Faller D, and Schubert J, et al (2011). The ZEB1/miR-200 feedback loop controls Notch signalling in cancer cells. *EMBO J* **30**, 770–782.

[4] Brabletz T (2012). EMT and MET in metastasis: where are the cancer stem cells? *Cancer Cell* **22**, 699–701.

[5] Preca BT, Bajdak K, Mock K, Sundararajan V, Pfannstiel J, Maurer J, Wellner U, Hopt UT, Brummer T, and Brabletz S, et al (2015). A self-enforcing CD44s/ZEB1 feedback loop maintains EMT and stemness properties in cancer cells. *Int J Cancer* **137**, 2566–2577.

[6] Bronsert P, Kohler I, Timme S, Kiefer S, Werner M, Schilling O, Vashist Y, Macowiec F, Brabletz T, and Hopt UT, et al (2014). Prognostic significance of Zinc finger E-box binding homeobox 1 (ZEB1) expression in cancer cells and cancer-associated fibroblasts in pancreatic head cancer. *Surgery* **156**, 97–108.

[7] Kim ST, Sohn I, Do IG, Jang J, Kim SH, Jung IH, Park JO, Park YS, Talasaz A, and Lee J, et al (2014). Transcriptome analysis of CD133-positive stem cells and prognostic value of surviving in colorectal cancer. *Cancer Genomics Proteomics* **11**, 259–266.

[8] Franco OE, Shaw AK, Strand DW, and Hayward SW (2009). Cancer associated fibroblasts in cancer pathogenesis. *Semin Cell Dev Biol* **2**, 33–39.

[9] Xing F, Saidou J, and Watabe K (2010). Cancer associated fibroblasts (CAFs) in tumor microenvironment. *Front Biosci (Landmark Ed)* **15**, 166–179.

[10] Apte MV, Xu Z, Pothula S, Goldstein D, Pirola RC, and Wilson JS (2015). Pancreatic cancer: the microenvironment needs attention too! *Pancreatology* **21**, 1424–3903.

[11] Wellner UF, Krauss T, Csanadi A, Lapshyn H, Bolm L, Timme S, Kulemann B, Hoeppner J, Kuesters S, and Seifert G, et al (2016). Mesopancreatic stromal clearance defines curative resection of pancreatic head cancer and can be predicted preoperatively by radiologic parameters: a retrospective study. *Medicine (Baltimore)* **95**, e2529.

[12] Rhim AD, Oberstein PE, Thomas DH, Mirek ET, Palermo CF, Sastra SA, Dekleva EN, Saunders T, Becerra CP, and Tattersall IW, et al (2014). Stromal elements act to restrain, rather than support, pancreatic ductal adenocarcinoma. *Cancer Cell* **25**, 735–747.

[13] Özdemir BC, Pentcheva-Hoang T, Carstens JL, Zheng X, Wu CC, Simpson TR, Laklai H, Sugimoto H, Kahlert C, and Novitskiy SV, et al (2014). Depletion of carcinoma-associated fibroblasts and fibrosis induces immunosuppression and accelerates pancreas cancer with reduced survival. *Cancer Cell* **25**, 719–734.

[14] Bosman FT, Carneiro F, Hruban RH, and Theise ND (2010). WHO Classification of Tumors of the Digestive System. 4th ed.Lyon: International Agency for Research in Cancer; 2010.

[15] Broders AC (1920). Squamous-cell epithelioma of the lip, a study of five hundred and thirty-seven cases. *JAMA* **74**, 656–664.

[16] Whright JR (2012). Broders' paradigm shifts involving the prognostication and definition of cancer. *Arch Pathol Lab Med*, 1437–1446.

[17] Ha SY, Yeo SY, Xuan YH, and Kim SH (2014). The prognostic significance of cancer-associated fibroblasts in esophageal squamous cell carcinoma. *PLoS One* **9**, e99955.

[18] Wellner U, Schubert J, Burk UC, Schmalhofer O, Zhu F, Sonntag A, Waldvogel B, Vannier C, Darling D, and zur Hausen A, et al (2009). The EMT-activator ZEB1 promotes tumorigenicity by repressing stemness-inhibiting microRNAs. *Nat Cell Biol* **11**, 1487–1495.

[19] Bronsert P, Enderle-Ammour K, Bader M, Timme S, Kuehs M, Csanadi A, Kayser G, Kohler I, Bausch D, and Hoeppner J, et al (2014). Cancer cell invasion and EMT marker expression: a three-dimensional study of the human cancer-host interface. *J Pathol* **234**, 410–422.

[20] Castello-Crós R and Cukierman R (2009). Stromagenesis during tumorigenesis: characterization of tumor-associated fibroblasts and stroma-derived 3D matrices. Extracellular Matrix Protocols2nd ed. 2009. p. 275–305.

[21] Zhan HX, Xu JW, Wang L, Zhang GY, and Hu SY (2015). Lymph node ratio is an independent prognostic factor for patients after resection of pancreatic cancer. *World J Surg Oncol* **13**, 105.

[22] Kim SH, Hwang HK, Lee WJ, and Kang CM (2016). Identification of an N staging system that predicts oncologic outcome in resected left-sided pancreatic cancer. *Medicine* **95**, e4035.

[23] Midwood KS, Williams LV, and Schwarzbauer JE (2004). Tissue repair and the dynamics of the extracellular matrix. *Int J Biochem Cell Biol* **36**, 1031–1037.

[24] Moffitt RA, Marayati R, Flate EL, Volmar KE, Loeza SGH, Hoadley KA, and Smyla JK (2015). Virtual microdissection identifies distinct tumor-and stroma-specific subtypes of pancreatic ductal adenocarcinoma. *Nat Genet* **47**, 1168–1178.

[25] Kalluri R (2016). The biology and function of fibroblasts in cancer. *Nat Rev Cancer* **16**, 582–598.

[26] Wilson JS, Pirola RC, and Apte MV (2014). Stars and stripes in pancreatic cancer: role of stellate cells and stroma in cancer progression. *Front Physiol* **14**, 52.

[27] Madar S, Goldstein I, and Rotter V (2013). 'Cancer associated fibroblasts'—more than meets the eye. *Trends Mol Med* **19**, 447–453.

[28] Aoki H, Ohnishi H, Hama K, Shinozaki S, Kita H, Yamamoto H, Osawa H, Sato K, Tamada K, and Sugano K (2006). Existence of autocrine loop between interleukin-6 and transforming growth factor-beta1 in activated rat pancreatic stellate cells. *J Cell Biochem* **99**, 221–228.

[29] Liotta LA and Kohn EC (2000). The microenvironment of the tumour-host interface. *Nature* **17**, 375–379.

[30] Bachem MG, Schünemann M, Ramadani M, Beger H, Buck A, Zhou S, Schmid-Kotsas A, and Adler G (2005). Pancreatic carcinoma cells induce fibrosis by stimulating proliferation and matrix synthesis of stellate cells. *Gastroenterology* **128**, 907–921.

[31] Apte MV, Park S, Phillips PA, Santucci N, Goldstein D, Kumar RK, Ramm GA, Buchler M, Friess H, and McCarroll JA, et al (2004). Desmoplastic reaction in pancreatic cancer: role of pancreatic stellate cells. *Pancreas* **29**, 179–187.

[32] Mckinney KQ, Lee JG, Sindram D, Russo MW, Han DK, Bonkovsky HL, and Hwang SI (2012). Identification of differentially expressed proteins from primary versus metastatic pancreatic cancer cells using subcellular proteomics. *Cancer Genomics Proteomics* **9**, 257–263.

[33] Brentnall TA, Lai LA, Coleman J, Bronner MP, Pan S, and Chen R (2012). Arousal of cancer-associated stroma: overexpression of palladin activates fibroblasts to promote tumor invasion. *PLoS One* **7**, e30219.

[34] Sukowati CHC, Anfuso B, Crocé LS, and Tiribelli C (2015). The role of multipotent cancer associated fibroblasts in hepatocarcinogenesis. *BMC Cancer* **15**, 1.

[35] Öhlund D, Handly-Santana A, Biffi G, Elyada E, Almeida AS, Ponz-Sarvise M, and Chio IIC (2017). Distinct populations of inflammatory fibroblasts and myofibroblasts in pancreatic cancer. *J Exp Med*.

[36] Moir JA, Mann J, and White SA (2015). The role of pancreatic stellate cells in pancreatic cancer. *Surg Oncol* **24**, 232–238.

[37] Brabletz T, Spaderna S, Kolb J, Hlubek F, Faller G, Bruns CJ, Jung A, Nentwich J, Duluc I, and Domon-Dell C, et al (2004). Down-regulation of the homeodomain factor Cdx2 in colorectal cancer by collagen type I. *Cancer Res* **64**, 6973–6977.

[38] Zhang L, Wu G, Herrle F, Niedergethmann M, and Keese M (2012). Single nucleotide polymorphisms of genes for EGF, TGF-β and TNF-α in patients with pancreatic carcinoma. *Cancer Genomics Proteomics* **9**, 287–295.

[39] Aigner K, Dampier B, Descovich L, Mikula M, Sultan A, Schreiber M, Mikulits W, Brabletz T, Strand D, and Obrist P, et al (2007). The transcription factor ZEB1 (δEF1) promotes tumour cell dedifferentiation by repressing master regulators of epithelial polarity. *Oncogene* **26**, 6979–6988.

[40] Arfmann-Knübel S, Struck B, Genrich G, Helm O, Sipos B, Sebens S, and Schäfer H (2015). The crosstalk between Nrf2 and TGF-β1 in the epithelial-mesenchymal transition of pancreatic duct epithelial cells. *PLoS One* **10**, e0132978.

[41] Lapshyn H, Bolm L, Kohler I, Werner M, Billmann FG, Bausch D, Hopt UT, Makowiec F, Wittel UA, and Keck T, et al (2017). Histopathological tumor invasion of the mesenterico-portal vein is characterized by aggressive biology and stromal fibroblast activation. *HPB (Oxford)* **19**, 67–74.

[42] Sousa CM and Kimmelman AC (2014). The complex landscape of pancreatic cancer metabolism. *Carcinogenesis* **35**, 1441–1450.

[43] Domper Arnal MJ, Ferrández Arenas Á, and Lanas Arbeloa Á (2015). Esophageal cancer: risk factors, screening and endoscopic treatment in Western and Eastern countries. *World J Gastroenterol* **14**, 7933–7943.